Published in IET Signal Processing
Received on 23rd August 2007
Revised on 19th April 2008
doi: 10.1049/iet-spr:20070162

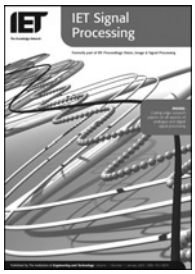


ISSN 1751-9675

# Efficient implementation of robust adaptive beamforming based on worst-case performance optimisation

*A. Elnashar*

*Emirates Integrated Telecommunications Company (du), Mobile Access Network, Technology Department, Dubai Media City, P.O. Box 502666, Dubai, UAE*
*E-mail: nashar_eg@yahoo.com*

**Abstract:** Traditional adaptive beamforming methods undergo serious performance degradation when a mismatch between the presumed and the actual array responses to the desired source occurs. Such a mismatch can be caused by desired look direction errors, distortion of antenna shape, scattering due to multipath, signal fading as well as other errors. This mismatch entails robust design of the adaptive beamforming methods. Here, the robust minimum variance distortionless response (MVDR) beamforming based on worst-case (WC) performance optimisation is efficiently implemented using a novel *ad hoc* adaptive technique. A new efficient implementation of the robust MVDR beamformer with a single WC constraint is developed. Additionally, the WC optimisation formulation is generalised to include multiple WC constraints which engender a robust linearly constrained minimum variance (LCMV) beamformer with multiple-beam WC (MBWC) constraints. Moreover, the developed LCMV beamformer with MBWC constraints is converted to a system of nonlinear equations and is efficiently solved using a Newton-like method. The first proposed implementation requires low computational complexity compared with the existing techniques. Furthermore, the weight vectors of the two developed adaptive beamformers are iteratively updated using iterative gradient minimisation algorithms which eliminate the estimation of the sample matrix inversion. Several scenarios including angle-of-incidence mismatch and multipath scattering with small and large angular spreads are simulated to study the robustness of the developed algorithms.

## 1 Introduction

Adaptive beamforming is a versatile approach to detect and estimate the signal of interest (SOI) at the output of a sensor array with applications in wireless communications, radar, sonar, astronomy, seismology, medical imaging and microphone array speech processing. Unfortunately, traditional adaptive array algorithms are known to be extremely sensitive even to slight mismatch between the presumed and the actual array responses to the desired signal [1]. Whenever a mismatch occurs, the adaptive beamformer inclines to misconstrue the SOI components in the array observations as interference and hence suppressing these components is most likely expected. The errors in array response to SOI can take place due to look directions errors, uncertainty in array sensor positions, mutual coupling, imperfect array calibration, multipath propagation due to local and remote scattering and limited sample support.

Many approaches have been proposed during the last two decades to improve the robustness of the traditional beamforming methods. A survey on these approaches can be found in [2, 3] and references therein. Among those approaches, the worst-case (WC) performance optimisation has been shown as a powerful technique which yields a beamformer with robustness against an arbitrary signal steering vector mismatch, data non-stationarity problems and small sample support [3–10]. The WC approach explicitly models an arbitrary (but bounded in norm)

mismatch in the desired signal array response and uses the WC performance optimisation to improve the robustness of the minimum variance distortionless response (MVDR) beamformer [5]. A theoretical analysis for this class of robust beamformers in terms of signal-to-interference-plus-noise ratio (SINR) in the presence of random steering vector errors is presented in [11, 12]. In addition, the closed-form expressions for the SINR are derived therein.

Unfortunately, the natural formulation of the WC performance optimisation involves the minimisation of a quadratic function subject to infinity non-convex quadratic constraints [5]. The approaches in [5, 6] reformulated the WC optimisation as a convex second-order cone program (SOCP) and solved it efficiently via the well-established interior point method [13]. Regrettably, the SOCP method does not provide a closed-form solution for the beamformer weights and even it cannot be implemented online, whereas the weight vector needs to be recomputed completely with the arrival of a new array observation [14–16].

Attractive approaches based on eigendecomposition of the sample covariance matrix have been introduced in [7–10]. These approaches developed a closed-form solution for a WC robust detector using the Lagrange method which incorporates the estimation of the norm of the weight vector and/or the Lagrange multiplier. A binary search algorithm followed by a Newton-like algorithm is proposed in [4, 8] to estimate the norm of the weight vector after dropping the Lagrange multiplier. Although these approaches have provided closed-form solutions for the WC beamformer, they, unfortunately, incorporate several difficulties. First, eigendecomposition for the sample covariance matrix is required with the arrival of a new array observation. Second, the inverse of diagonally loaded sample covariance matrix is required to estimate the weight vector. Third, some difficulties are encountered during algorithm initialisation and a stopping criterion is necessary to prevent negative solution of the Newton-like algorithm.

In this paper, two efficient *ad hoc* implementations of the WC performance optimisation problem are adopted. First, the robust MVDR beamformer with a single WC constraint is implemented using an iterative gradient minimisation algorithm with an *ad hoc* technique to estimate the Lagrange multiplier instead of the Newton-like algorithm. The proposed algorithm exhibits several merits including simplicity, low computational load and no need for either sample-matrix inversion or eigendecomposition. A geometric interpretation of the proposed implementation is introduced to supplement the theoretical analysis. Second, a robust linearly constrained minimum variance (LCMV) beamformer with multiple-beam WC (MBWC) constraints is developed using a novel multiple WC constraints formulation. The Lagrange method is exploited to solve this optimisation problem, which reveals that the solution of the robust LCMV beamformer with MBWC constraints entails solving a set of nonlinear equations. As a consequence, a Newton-like method is mandatory to solve the ensuing system of nonlinear equations which yields a vector of Lagrange multipliers. It is worthwhile to note that the approaches in [15, 17] adopt *ad hoc* techniques to optimise the beamformer output power with spherical constraint on the steering vector. Unfortunately, the adaptive beamformer developed in [17] is apt to noise enhancement at low SNR and additional constraint is required to bear the ellipsoidal constraint [15].

The rest of the paper is organised as follows. In Section 2, the standard MVDR and LCMV beamformers with single and multiple constraints are summarised in the context of a single point source and a source with multipath rays, respectively. In Section 3, the WC optimisation formulation is introduced by summarising general and special formulations for the steering vector uncertainty set. Efficient implementations of single and multiple WC formulations are derived and analysed in Section 4 and Section 5, respectively. Moreover, a geometric illustration for the single WC implementation is presented. Simulations and performance analysis are provided in Section 6. Conclusions and points for future work are encapsulated in Section 7.

## 2 Standard beamforming methods

Consider an array comprising $M$ uniformly spaced sensors receives a narrowband signal $\boldsymbol{s}_{\mathrm{d}}(k)$. Initially, it is assumed that the desired signal is a point source with time-invariant wavefront, and the $M \times 1$ vector of array observations can be modelled as [2–5]

$$\boldsymbol{x}(k) = \boldsymbol{a}_{\mathrm{d}}(\varphi)s_{\mathrm{d}}(k) + \boldsymbol{i}(k) + \boldsymbol{n}(k) \tag{1}$$

where $k$ is the time index, $s_{\mathrm{d}}(k)$ the complex signal waveform of the desired signal and $\boldsymbol{a}_{\mathrm{d}}(\varphi)$ its $M \times 1$ steering vector where $\varphi$ is the angle of incidence (AOI) and $\boldsymbol{i}(k)$ and $\boldsymbol{n}(k)$ the statically independent components of the interference and the noise, respectively.

A generalised model with multipath propagation can be expressed as follows

$$\boldsymbol{x}(k) = s_{\mathrm{d}}(k)\sum_{n=1}^{L}\gamma_n\boldsymbol{a}_{\mathrm{d}}(\varphi+\phi_n) + \boldsymbol{i}(k) + \boldsymbol{n}(k) \tag{2}$$

where $L$ is the number of multipaths with each path has a random complex gain $\gamma_n$ and an angular deviation $\phi_n$ from the nominal AOI $\varphi$. The scattered signals associated with the multipath propagation from a single source arrive at the base station (BS) from several directions within an angular region called the angular spread. The angular spread arises due to the multipath, both from local scatters near to the source and near to the BS and from remote scatters.



*IET Signal Process.*, 2008, Vol. 2, No. 4, pp. 381–393
doi: 10.1049/iet-spr:20070162

It varies according to the cell morphological type (i.e. dense urban, urban and rural), cell radius, BS location and antenna height. It can vary from few degrees at rural road cells to 360° in microcellular and indoor environment due to the reflecting surfaces surround the BS antenna. It is assumed that the time delays of the different multipath components are small compared with the inverse of the signal bandwidth (i.e. narrowband channel model) and therefore the delay can be modelled as a phase shift in the complex gain $\gamma_n$ [18]. The angular spread is used here to describe the angular region associated with the entire multipaths. Notwithstanding each of the rays itself may be composed of a large number of 'mini-rays' with roughly equal angles and delays but with arbitrary phases due to scattering close to the source [19]. In this paper, the model is simplified by using the nominal AOI of each ray group and multipath delays are modelled as a small angle in the complex gain.

The beamformer output signal can be written as

$$y(k) = \boldsymbol{w}^{\mathrm{H}}(k)\boldsymbol{x}(k) \tag{3}$$

where $\boldsymbol{x}(k) = \left[\, x_1(k), \ldots, x_M(k) \,\right]^{\mathrm{T}}$ is an $M \times 1$ complex vector of the array observations, $\boldsymbol{w}(k) = \left[\, w_1(k), \ldots, w_M(k) \,\right]^{\mathrm{T}}$ is an $M \times 1$ complex vector of the beamformer weights and $(\cdot)^{\mathrm{T}}$ and $(\cdot)^{\mathrm{H}}$ stand for the transpose and Hermitian transpose, respectively.

Consider the simplified model in (1) with the point source. The optimal weight vector seeks maximisation of the output SINR [3–5, 10, 11]

$$\mathrm{SINR} = \frac{\sigma_{\mathrm{d}}^2 \left| \boldsymbol{w}^{\mathrm{H}} \boldsymbol{a}_{\mathrm{d}} \right|^2}{\boldsymbol{w}^{\mathrm{H}} \boldsymbol{R}_{i+n} \boldsymbol{w}} \tag{4}$$

where $\boldsymbol{R}_{i+n} \triangleq E\left\{ (\boldsymbol{i}(k) + \boldsymbol{n}(k))(\boldsymbol{i}(k) + \boldsymbol{n}(k))^{\mathrm{H}} \right\}$ is the interference-plus-noise covariance matrix and $\sigma_{\mathrm{d}}^2$ is the desired source power. The optimal solution of $\boldsymbol{w}$ which maximises the output SINR in (4) can be obtained by maintaining distortionless response to the desired source while minimising the output interference-plus-noise power (i.e. $\boldsymbol{w}^{\mathrm{H}} \boldsymbol{R}_{i+n} \boldsymbol{w}$). In practical applications, the interference-plus-noise covariance matrix can be replaced by the sample covariance matrix [2–10], which can be estimated using the first-order recursion

$$\widehat{\boldsymbol{R}}(n) = \sum_{i=1}^{n} \eta^{n-i} \boldsymbol{x}(i) \boldsymbol{x}^{\mathrm{H}}(i) = \eta \widehat{\boldsymbol{R}}(n-1) + \boldsymbol{x}(n) \boldsymbol{x}^{\mathrm{H}}(n) \tag{5}$$

where $\eta$ is a forgetting factor which satisfies $0 \ll \eta \leq 1$.

The minimum variance beamformer with single-beam constraint (SBC) can be formulated as follows

$$\begin{aligned} \min_{\boldsymbol{w}} \quad & \boldsymbol{w}^{\mathrm{H}} \widehat{\boldsymbol{R}} \boldsymbol{w} \\ \text{subject to} \quad & \boldsymbol{w}^{\mathrm{H}} \boldsymbol{a}_{\mathrm{d}} = 1 \end{aligned} \tag{6}$$

The solution of (6) engenders the standard MVDR beamformer with SBC and can be easily derived as

$$\boldsymbol{w}_{\mathrm{SBC}} = \frac{\widehat{\boldsymbol{R}}^{-1} \boldsymbol{a}_{\mathrm{d}}}{\boldsymbol{a}_{\mathrm{d}}^{\mathrm{H}} \widehat{\boldsymbol{R}}^{-1} \boldsymbol{a}_{\mathrm{d}}} \tag{7}$$

Considering the generalised received signal model in (2), the optimum MVDR beamformer can be obtained using multiple constraints to provide multiple-beam constraint (MBC) beamformer, that is

$$\begin{aligned} \min_{\boldsymbol{w}} \quad & \boldsymbol{w}^{\mathrm{H}} \widehat{\boldsymbol{R}} \boldsymbol{w} \\ \text{subject to} \quad & \boldsymbol{w}^{\mathrm{H}} \Lambda(\boldsymbol{\theta}_0) = \boldsymbol{v} \end{aligned} \tag{8}$$

where $\boldsymbol{\theta}_0 = \left[\, \theta_1 \cdots \theta_L \,\right]$ and $\boldsymbol{\Lambda}(\boldsymbol{\theta}_0) = \left[\, \boldsymbol{a}(\theta_1) \cdots \boldsymbol{a}(\theta_L) \,\right]$ is the $M \times L$ spatial constraint matrix consists of the steering vectors corresponding to the AOIs of the multipath rays associated with the desired source and $\boldsymbol{v}$ is a vector of the constrained values (i.e. gain vector) which can all be set to one for equal gain combining or alternatively it can be optimised using maximal ratio combining (MRC) technique. Accordingly, the optimal weight vector of (8), termed as the LCMV beamformer, is given by [10]

$$\boldsymbol{w}_{\mathrm{MBC}} = \widehat{\boldsymbol{R}}^{-1} \Lambda \left( \Lambda^{\mathrm{H}} \widehat{\boldsymbol{R}}^{-1} \Lambda \right)^{-1} \boldsymbol{v} \tag{9}$$

## 3 Robust adaptive MVDR beamformer with single WC constraint

The beamforming formulations in (6) and (8) assume that the array response to the desired source (i.e. the steering vector $\boldsymbol{a}_{\mathrm{d}}$ of the point source or the spatial matrix $\Lambda$ of a source with multipath rays) is precisely known. However, practically, the knowledge of the desired source steering vector or spatial matrix may be imprecise. In this paper, the recently emerged rigorous approach to robust MVDR beamforming based on the WC performance optimisation [3–10] is considered.

First consider the formulation of the standard MVDR beamformer in (6) with SBC, and following the approaches in [5–10], to add robustness to the standard MVDR

beamformer in (7), the WC weighted power output of the array is minimised in the presence of uncertainties in the steering vector, that is

$$\begin{aligned} \min_{\boldsymbol{w}} \quad & \boldsymbol{w}^{\mathrm{H}}\widehat{\boldsymbol{R}}\boldsymbol{w} \\ \text{subject to} \quad & \left|\boldsymbol{w}^{\mathrm{H}}\boldsymbol{z}\right| \geq 1 \quad \forall \boldsymbol{z} \in \varepsilon \end{aligned} \tag{10}$$

where $\varepsilon$ is an ellipsoid that covers the possible range of the imprecise steering vector $\boldsymbol{z}$. Assuming $\varepsilon$ is centred at the presumed steering vector $\boldsymbol{a}_{\mathrm{d}}$ [10], that is

$$\varepsilon = \left\{\boldsymbol{A}\boldsymbol{u} + \boldsymbol{a}_{\mathrm{d}} | \|\boldsymbol{u}\| \leq 1\right\} \tag{11}$$

where the matrix $\boldsymbol{A}$ determines the size and shape of the ellipsoid $\varepsilon$. If $\boldsymbol{A} = \zeta \boldsymbol{I}$ [5–8] is set, the following special case of $\varepsilon$ is obtained

$$\varepsilon = \left\{\boldsymbol{e} + \boldsymbol{a}_{\mathrm{d}} | \|\boldsymbol{e}\| \leq \zeta\right\}, \quad \boldsymbol{e} = \zeta \boldsymbol{u} \tag{12}$$

Assuming that $\widehat{\boldsymbol{R}}$ in (10) is a positive definite matrix and then the optimisation problem in (10) along with the generalised ellipsoid in (11) can be converted to the following form [10]

$$\begin{aligned} \min_{\boldsymbol{w}} \quad & \boldsymbol{w}^{\mathrm{H}}\widehat{\boldsymbol{R}}\boldsymbol{w} \\ \text{subject to} \quad & \left|\boldsymbol{w}^{\mathrm{H}}\boldsymbol{a}_{\mathrm{d}}\right| \geq \left\|\mathbf{A}^{\mathrm{H}}\boldsymbol{w}\right\| + 1 \end{aligned} \tag{13}$$

Likewise, the optimisation problem in (10) with the WC constraint in (12) can be expressed as [5]

$$\begin{aligned} \min_{\boldsymbol{w}} \quad & \boldsymbol{w}^{\mathrm{H}}\widehat{\boldsymbol{R}}\boldsymbol{w} \\ \text{subject to} \quad & \left|\boldsymbol{w}^{\mathrm{H}}\boldsymbol{a}_{\mathrm{d}}\right| \geq \zeta\|\boldsymbol{w}\| + 1 \end{aligned} \tag{14}$$

Unfortunately, the nonlinear constraints in (13) and (14) are non-convex due to the absolute value function on the left-hand side. Indeed, the cost functions in (13) and (14) are unchanged when $\boldsymbol{w}$ undergoes an arbitrary phase rotation [5–10]. As a consequence, with the optimal solutions of (13) and (14), it can always rotate without affecting the cost function optimisation. Therefore the optimal solution may be chosen, without loss of generality, such that

$$\mathrm{Re}\left\{\boldsymbol{w}^{\mathrm{H}}\boldsymbol{a}_{\mathrm{d}}\right\} \geq 0 \tag{15}$$

$$\mathrm{Im}\left\{\boldsymbol{w}^{\mathrm{H}}\boldsymbol{a}_{\mathrm{d}}\right\} = 0 \tag{16}$$

Using (15) and (16), the optimisation problems in (13) and (14) can be converted to the following convex formulations, respectively, [10] and [5]

$$\begin{aligned} \min_{\boldsymbol{w}} \quad & \boldsymbol{w}^{\mathrm{H}}\widehat{\boldsymbol{R}}\boldsymbol{w} \\ \text{subject to} \quad & \boldsymbol{w}^{\mathrm{H}}\boldsymbol{a}_{\mathrm{d}} \geq \left\|\boldsymbol{A}^{\mathrm{H}}\boldsymbol{w}\right\| + 1 \end{aligned} \tag{17}$$

$$\begin{aligned} \min_{\boldsymbol{w}} \quad & \boldsymbol{w}^{\mathrm{H}}\widehat{\boldsymbol{R}}\boldsymbol{w} \\ \text{subject to} \quad & \boldsymbol{w}^{\mathrm{H}}\boldsymbol{a}_{\mathrm{d}} \geq \zeta\|\boldsymbol{w}\| + 1 \end{aligned} \tag{18}$$

The constraints in (17) and (18) are called second-order cone constraints. Two SOCP approaches are proposed in [6] and [5] for real and complex formulations, respectively.

## 3.1 Lagrange approach

First form the following Lagrange function

$$J(\boldsymbol{w}, \lambda) = \boldsymbol{w}^{\mathrm{H}}\widehat{\boldsymbol{R}}\boldsymbol{w} - \lambda t\left(\boldsymbol{w}^{\mathrm{H}}\boldsymbol{a}_{\mathrm{d}} - \zeta\|\boldsymbol{w}\| - 1\right) \tag{19}$$

where $t(\cdot)$ is a step function guarantees that $\boldsymbol{w}^{\mathrm{H}}\boldsymbol{a}_{\mathrm{d}} \geq \zeta|\boldsymbol{w}| + 1$ and $\lambda$ is the Langrage multiplier. The inequality constraint in (18) is satisfied by equality if the cost function in (19) is minimised. This fact can be proved by contradiction [4, 8] and hence the step function in (19) is dispensable. By differentiating (19) and equating the result to zero, one has [4]

$$\widehat{\boldsymbol{R}}\boldsymbol{w} + \lambda\zeta\frac{\boldsymbol{w}}{\|\boldsymbol{w}\|} = \lambda\boldsymbol{a}_{\mathrm{d}} \tag{20}$$

By solving for $\boldsymbol{w}$, the following closed-form solution is obtained

$$\boldsymbol{w}_{\mathrm{WC}} = \lambda\left(\widehat{\boldsymbol{R}} + \frac{\lambda\zeta}{\|\boldsymbol{w}_{\mathrm{WC}}\|}\boldsymbol{I}\right)^{-1}\boldsymbol{a}_{\mathrm{d}} \tag{21}$$

The WC Robust MVDR beamformer in (21) encompasses three difficulties as follows: the estimation of the weight vector norm, the estimation of the Lagrange multiplier which achieves (21) and the computational load of computing the inverse of the diagonally loaded sample covariance matrix. In the following two sections, two techniques are summarised for computing $\boldsymbol{w}_{\mathrm{WC}}$.

*3.1.1 Eigendecomposition method:* Several eigen decomposition approaches have been developed to solve the WC performance optimisation problem. The optimisation problems in (17) and (18) have been solved, respectively, in [10] and [4, 8] using eigendecomposition methods. For the sake of comparison, the approach in [4, 8] is briefly reviewed. Using the fact that multiplying $\boldsymbol{w}_{\mathrm{WC}}$ in (20) by any arbitrary constant does not affect the bit error rate performance of the beamformer [4, 8], a scaled version of




doi: 10.1049/iet-spr:20070162

the WC beamformer can be obtained as follows [4]

$$\tilde{\boldsymbol{w}}_{\mathrm{WC}} = \left(\widehat{\boldsymbol{R}} + \frac{\zeta}{\|\tilde{\boldsymbol{w}}_{\mathrm{WC}}\|}\boldsymbol{I}\right)^{-1}\boldsymbol{a}_{\mathrm{d}} \tag{22}$$

A binary search algorithm followed by Newton–Raphson iterations is proposed in [8] to compute the norm of the WC beamformer $\|\tilde{\boldsymbol{w}}_{\mathrm{WC}}\|$. The eigendecomposition approach accurately estimates the norm of the robust detector $\|\tilde{\boldsymbol{w}}_{\mathrm{WC}}\|$ and hence the optimal weight vector can be obtained using the closed form in (22).

*3.1.2 Taylor series approximation method:* By applying the Taylor series expansion to (22) analogous to the approach in [20], the following

$$\begin{aligned}\tilde{\boldsymbol{w}}_{\mathrm{WC}} &= \left(\boldsymbol{I} + \frac{\zeta}{\|\tilde{\boldsymbol{w}}_{\mathrm{WC}}\|}\widehat{\boldsymbol{R}}^{-1}\right)^{-1}\widehat{\boldsymbol{R}}^{-1}\boldsymbol{a}_{\mathrm{d}} \\ &\simeq \bar{\boldsymbol{w}}_{\mathrm{SBC}} - \frac{\zeta}{\|\tilde{\boldsymbol{w}}_{\mathrm{WC}}\|}\widehat{\boldsymbol{R}}^{-1}\bar{\boldsymbol{w}}_{\mathrm{SBC}}\end{aligned} \tag{23}$$

is obtained, where $\bar{\boldsymbol{w}}_{\mathrm{SBC}} = \widehat{\boldsymbol{R}}^{-1}\boldsymbol{a}_{\mathrm{d}}$ is a biased version of the standard MVDR beamformer in (7). By introducing a new vector $\tilde{\boldsymbol{w}}_{\mathrm{SBC}} = \widehat{\boldsymbol{R}}^{-1}\bar{\boldsymbol{w}}_{\mathrm{SBC}}$ and substituting into (23) yield

$$\tilde{\boldsymbol{w}}_{\mathrm{WC}} \simeq \bar{\boldsymbol{w}}_{\mathrm{SBC}} - \kappa\tilde{\boldsymbol{w}}_{\mathrm{SBC}} \tag{24}$$

where $\kappa = \zeta/\|\tilde{\boldsymbol{w}}_{\mathrm{WC}}\|$ is a parameter related to the weight vector norm of the WC robust beamformer and can be estimated by plugging (24) into the WC constraint in (18). This approach is almost similar to the eigendecomposition approach where low complexity is introduced at the expense of the weight vector norm estimation accuracy owing to Taylor series approximation.

# 4 Efficient implementation of robust adaptive MVDR beamformer with single WC constraint

In this section, efficient adaptive implementations of robust adaptive MVDR beamformer based on WC performance optimisation is developed. The WC performance optimisation MVDR beamforming is efficiently implemented using iterative gradient minimisation algorithm with *ad hoc* technique to satisfy the WC constraint.

The adaptive beamformer can be found by searching for a weight vector $\boldsymbol{w}$ that minimises the cost function (19). In order to find the target beamformer in an iterative manner, the weight vector can be updated as follows

$$\boldsymbol{w}(k+1) = \boldsymbol{w}(k) - \mu(k)\nabla(k) \tag{25}$$

where $k$ is the snapshot index, $\nabla(k)$ the gradient vector of the Lagrange function $J(\boldsymbol{w}, \lambda)$ in (19) with respect to $\boldsymbol{w}$ determined at snapshot $k$ and $\mu(k)$ an adaptive step size which determines the convergence speed of the algorithm.

The gradient vector of the cost function in (19) is given by

$$\nabla = \frac{\partial J(\boldsymbol{w}, \lambda)}{\partial \boldsymbol{w}} = \widehat{\boldsymbol{R}}\boldsymbol{w} - \lambda\left(\frac{\boldsymbol{a}_{\mathrm{d}} - \zeta\boldsymbol{w}}{\|\boldsymbol{w}\|}\right) \tag{26}$$

The step function is dropped due to *ad hoc* adaptive implementation. Hence, the adaptive weight vector can be obtained by substituting (26) into (25), which yields

$$\begin{aligned}\boldsymbol{w}(k+1) = \boldsymbol{w}(k) &- \mu(k)\widehat{\boldsymbol{R}}(k)\boldsymbol{w}(k) \\ &+ \mu(k)\lambda\left(\frac{\boldsymbol{a}_{\mathrm{d}} - \zeta\boldsymbol{w}(k)}{\|\boldsymbol{w}(k)\|}\right)\end{aligned} \tag{27}$$

For simplicity, two new vectors are introduced: $\widehat{\boldsymbol{w}}(k+1) = \boldsymbol{w}(k) - \mu(k)\widehat{\boldsymbol{R}}(k)\boldsymbol{w}(k)$ (referred to as unconstrained MV weight vector) and $\boldsymbol{\pi}(k) = \boldsymbol{a}_{\mathrm{d}} - \zeta\boldsymbol{w}(k)/\|\boldsymbol{w}(k)\|$. Therefore the weight vector of the robust WC adaptive beamformer can be updated as follows

$$\boldsymbol{w}(k+1) = \widehat{\boldsymbol{w}}(k+1) + \mu(k)\lambda\boldsymbol{\pi}(k) \tag{28}$$

## 4.1 Lagrange multiplier estimation

We assume that the weight vector $\boldsymbol{w}(k)$ satisfies the WC constraint in (18) and then, $\boldsymbol{w}(k+1)$ should also satisfy the WC constraint. The weight vector $\widehat{\boldsymbol{w}}(k+1)$ represents the minimisation of the unconstrained MV cost function (i.e. $\boldsymbol{w}^{\mathrm{H}}\widehat{\boldsymbol{R}}\boldsymbol{w}$) which leads to trivial zero solution if the additional WC constraint is not imposed. In order to fully satisfy the inequality constraint in (18), first the weight vector $\widehat{\boldsymbol{w}}(k+1)$ is computed and then it is verified if $\widehat{\boldsymbol{w}}(k+1)$ achieves the WC constraint in (18). Consequently, if $\widehat{\boldsymbol{w}}(k+1)$ satisfies the WC constraint, the weight vector is accepted and the algorithm continues with a new array observation. Otherwise, (28) is substituted into the inequality constraint in (18) to estimate the Lagrange multiplier as follows

$$\begin{aligned}&\mathrm{Re}\left\{\left(\widehat{\boldsymbol{w}}(k+1) + \mu(k)\lambda\boldsymbol{\pi}(k)\right)^{\mathrm{H}}\boldsymbol{a}_{\mathrm{d}}\right\} \\ &\quad\geq \zeta\left\|\left(\widehat{\boldsymbol{w}}(k+1) + \mu(k)\lambda\boldsymbol{\pi}(k)\right)\right\| + 1\end{aligned} \tag{29}$$

where $\mathrm{Re}\{\bullet\}$ is inserted to make sure that (15) and (16) are always guaranteed during adaptive implementation. After arranging and boosting both sides of (29) to the power of two

$$\begin{aligned}&\left(\mathrm{Re}\left\{\left(\widehat{\boldsymbol{w}}(k+1) + \mu(k)\lambda\boldsymbol{\pi}(k)\right)^{\mathrm{H}}\boldsymbol{a}_{\mathrm{d}}\right\} - 1\right)^2 \\ &\quad\geq \zeta^2\left\|\left(\widehat{\boldsymbol{w}}(k+1) + \mu(k)\lambda\boldsymbol{\pi}(k)\right)\right\|^2\end{aligned} \tag{30}$$

is obtained.

By rearranging (30), one has

$$\left(\left(\mathrm{Re}\left\{\widehat{\boldsymbol{w}}(k+1)^{\mathrm{H}}\boldsymbol{a}_{\mathrm{d}}\right\}-1\right)+\mu(k)\lambda\mathrm{Re}\left\{\boldsymbol{\pi}(k)^{\mathrm{H}}\boldsymbol{a}_{\mathrm{d}}\right\}\right)^2 \geq \zeta^2\left(\widehat{\boldsymbol{w}}(k+1)+\mu(k)\lambda\boldsymbol{\pi}(k)\right)^{\mathrm{H}}\left(\widehat{\boldsymbol{w}}(k+1)+\mu(k)\lambda\boldsymbol{\pi}(k)\right) \tag{31}$$

The Lagrange multiplier $\lambda$ which achieves the WC constraint in (18) needs to be estimated. During the *ad hoc* implementation, (31) will be solved only if the WC constraint is not met. Following this fact, the inequality in (31) is replaced by equality and after some manipulations to (31), one has

$$\chi^2+2\mu(k)\lambda\chi\boldsymbol{\pi}(k)^{\mathrm{H}}\boldsymbol{a}_{\mathrm{d}}+\mu(k)^2\lambda^2\left(\boldsymbol{\pi}(k)^{\mathrm{H}}\boldsymbol{a}_{\mathrm{d}}\right)^2 = \zeta^2\left\|\widehat{\boldsymbol{w}}(k+1)\right\|^2+2\mu(k)\zeta^2\lambda\mathrm{Re}\left\{\boldsymbol{\pi}(k)^{\mathrm{H}}\widehat{\boldsymbol{w}}(k+1)\right\} +\mu(k)^2\zeta^2\lambda^2\|\boldsymbol{\pi}(k)\|^2 \tag{32}$$

where $\chi=\mathrm{Re}\left\{\widehat{\boldsymbol{w}}(k+1)^{\mathrm{H}}\boldsymbol{a}_{\mathrm{d}}\right\}-1$.

Therefore the Lagrange multiplier $\lambda$ can be computed as the solution to the following quadratic equation

$$\mu(k)^2\lambda^2\left(\left(\mathrm{Re}\left\{\boldsymbol{\pi}(k)^{\mathrm{H}}\boldsymbol{a}_{\mathrm{d}}\right\}\right)^2-\zeta^2\|\boldsymbol{\pi}(k)\|^2\right) +2\mu(k)\lambda\left(\chi\mathrm{Re}\left\{\boldsymbol{\pi}(k)^{\mathrm{H}}\boldsymbol{a}_{\mathrm{d}}\right\}-\zeta^2\mathrm{Re}\left\{\boldsymbol{\pi}(k)^{\mathrm{H}}\widehat{\boldsymbol{w}}(k+1)\right\}\right) +\chi^2-\zeta^2\left\|\widehat{\boldsymbol{w}}(k+1)\right\|^2=0 \tag{33}$$

Therefore the value of $\lambda$ which achieves the WC constraint in (18) has the following form

$$\lambda=-B\pm\sqrt{\frac{B^2-AC}{A}} \tag{34}$$

where

$$A=\mu(k)^2\left(\left(\mathrm{Re}\left\{\boldsymbol{\pi}(k)^{\mathrm{H}}\boldsymbol{a}_{\mathrm{d}}\right\}\right)^2-\zeta^2\|\boldsymbol{\pi}(k)\|^2\right)$$
$$B=\mu(k)\left(\chi\mathrm{Re}\left\{\boldsymbol{\pi}(k)^{\mathrm{H}}\boldsymbol{a}_{\mathrm{d}}\right\}-\zeta^2\mathrm{Re}\left\{\boldsymbol{\pi}(k)^{\mathrm{H}}\widehat{\boldsymbol{w}}(k+1)\right\}\right)$$
$$C=\chi^2-\zeta^2\left\|\widehat{\boldsymbol{w}}(k+1)\right\|^2 \tag{35}$$

The Lagrange multiplier estimation is merely executed when the WC constraint is not achieved, that is, $\chi<\zeta\left\|\widehat{\boldsymbol{w}}(k+1)\right\|$. Therefore $C<0$ and the roots of (33) fall under one of the following categories.

- $A>0$ and $B>0$:
Equation (33) has two real roots: one positive root and one negative root resulting from positive and minus signs in (34), respectively. The positive root is selected to make sure that $\left(\widehat{\boldsymbol{R}}+\lambda\zeta/\|\boldsymbol{w}_{\mathrm{RMV}}\|\boldsymbol{I}\right)^{-1}$ is a positive definite matrix.

- $A<0$ and $B>0$:
Equation (33) has only one real positive root resulting from positive sign in (34) if $B^2>AC$.

- $A>0$ and $B<0$:
Therefore (33) has two positive real solutions. In this case, the smaller root is selected to guarantee algorithm stability.

- $A<0$ and $B<0$:
Equation (33) is guaranteed to have one real positive solution if $B^2>AC$.

## 4.2 Recursive implementation

The optimum step size of minimising $\boldsymbol{w}^H\widehat{\boldsymbol{R}}\boldsymbol{w}$ is the best estimate to the optimum step size which minimises (19). As a consequence, the optimum step size can be obtained by substituting (25) into (19) and differentiating with respect to the adaptive step size, then equating the result to zero, the following optimum step size is obtained [15, 21, 22]

$$\mu_{\mathrm{opt}}(k)=\left.\frac{\alpha\widehat{\nabla}^{\mathrm{H}}(k)\widehat{\nabla}(k)}{\widehat{\nabla}^{\mathrm{H}}(k)\widehat{\boldsymbol{R}}(k)\widehat{\nabla}(k)}\right|_{\widehat{\nabla}=\widehat{\boldsymbol{R}}(k)\boldsymbol{w}(k)} \tag{36}$$

The parameter $\alpha$ is added to improve the numerical stability of the algorithm. For a practical system, it should be adjusted during initial tuning of the system and it should satisfy $0<\alpha<1$ [21, 22].

To summarise, the proposed WC robust adaptive beamformer algorithm consists of the following steps.

*Step 0.* Initialise: $\widehat{\boldsymbol{R}}(0)=\boldsymbol{I}$, $\boldsymbol{w}(0)=\boldsymbol{a}_{\mathrm{d}}$, $\alpha=0.1$, $\eta=0.97$

*Step 1.* Pick a new sample from array observations and compute the sample covariance matrix: $\widehat{\boldsymbol{R}}(k)=\eta\widehat{\boldsymbol{R}}(k-1)+\boldsymbol{x}(k)\boldsymbol{x}^{\mathrm{H}}(k)$; $M^2$.

*Step 2.* Compute the optimum step-size using (36); $M^2+2M$.

*Step 3.* Update the unconstrained MV weight vector: $\widehat{\boldsymbol{w}}(k+1)=\boldsymbol{w}(k)-\mu(k)\widehat{\boldsymbol{R}}(k)\boldsymbol{w}(k)$; the matrix vector multiplication $\widehat{\boldsymbol{R}}(k)\boldsymbol{w}(k)$ is computed in step 2.

*Step 4.* If $\chi<\zeta\left\|\widehat{\boldsymbol{w}}(k+1)\right\|$ compute $\lambda$ using (34); $5M$.
Else $\lambda=0$ and $\boldsymbol{w}(k+1)=\widehat{\boldsymbol{w}}(k+1)\rightarrow$ go to step 1.

*Step 5.* Update the WC weight vector as: $\boldsymbol{w}(k+1)=\widehat{\boldsymbol{w}}(k+1)+\mu(k)\lambda\boldsymbol{\pi}(k)\rightarrow$ go to step 1.

As shown in the above implementation, the total multiplications complexity of the proposed algorithm is about $O(2M^2+7M)$. More interestingly, the WC




doi: 10.1049/iet-spr:20070162

optimisation step with the *ad hoc* implementation requires $O(M)$ complexity while it requires $O(M^3)$ using SOCP, and in the eigendecomposition method, the estimation of the norm vector of the WC weight vector requires $O(M^3)$ alone [3–8].

### 4.3 Geometric interpretation of the proposed WC beamformer

In order to further illustrate the proposed algorithm, it is exemplified using a geometric interpretation. Fig. 1 represents the geometric illustration for the proposed WC adaptive beamforming implementation using simple 2D case similar to the approach in [23]. The vector $\overrightarrow{OA}$ represents the presumed steering vector $\boldsymbol{a}_{\mathrm{d}}$. The vector $\overrightarrow{OB}$ represents the WC robust beamformer at snapshot $k$. The concentric ellipses represent the unconstrained MV cost function, that is, $\boldsymbol{w}^{\mathrm{H}}\widehat{\boldsymbol{R}}\boldsymbol{w}$ and the centre of these ellipses is the minimal point (i.e. trivial zero solution) that minimises this cost function. Assuming that the WC weight vector $\boldsymbol{w}(k)$ satisfies the WC constraint, that is, $\overrightarrow{OB}^{\mathrm{H}}\overrightarrow{OA} \geq \zeta\left\|\overrightarrow{OB}\right\| + 1$. The forthcoming update of the unconstrained MV weight vector is computed as $\widetilde{\boldsymbol{w}}(k+1) = \boldsymbol{w}(k) - \mu(k)\widehat{\boldsymbol{R}}(k)\boldsymbol{w}(k)$, that is, $\overrightarrow{OC} = \overrightarrow{OB} + \overrightarrow{BC}$. As depicted in Fig. 1, the vector $\overrightarrow{BC}$ represents the gradient of the MV cost function, that is, $-u(k)\widehat{\boldsymbol{R}}(k)\boldsymbol{w}(k)$, which is perpendicularly inward inside the contours and towards the centre of the ellipsis. When the subsequent vector $\overrightarrow{OC}$ does not satisfy the WC constraint (i.e. $\overrightarrow{OC}^{\mathrm{H}}\overrightarrow{OA} < \zeta\left\|\overrightarrow{OC}\right\| + 1$), the condition in the step 4 in the algorithm is met, and subsequently, the vector $\overrightarrow{AE} = -\zeta\boldsymbol{w}(k)/\|\boldsymbol{w}(k)\|$, which parallel to the vector $\overrightarrow{BO}$, is added to $\overrightarrow{OA}$ to estimate $\boldsymbol{\pi}(k)$ (i.e. $\overrightarrow{OE} = \overrightarrow{OA} + \overrightarrow{AE}$). Then, the WC weight vector $\overrightarrow{OD} = \boldsymbol{w}(k+1)$ is generated by adding the vector $\overrightarrow{CD} = \mu(k)\lambda\boldsymbol{\pi}(k)$, which is parallel to the vector $\overrightarrow{OE}$, to the vector $\overrightarrow{OC}$, (i.e. $\overrightarrow{OD} = \overrightarrow{OC} + \overrightarrow{CD}$). Consequently, the ensuing weight vector $\overrightarrow{OD}$ satisfies the WC constraint. In a nutshell, the WC constraint prevents the weight vector from reaching the trivial zero solution by maintaining distortionless response to a set of possible steering vectors which is controlled by the WC constraint.

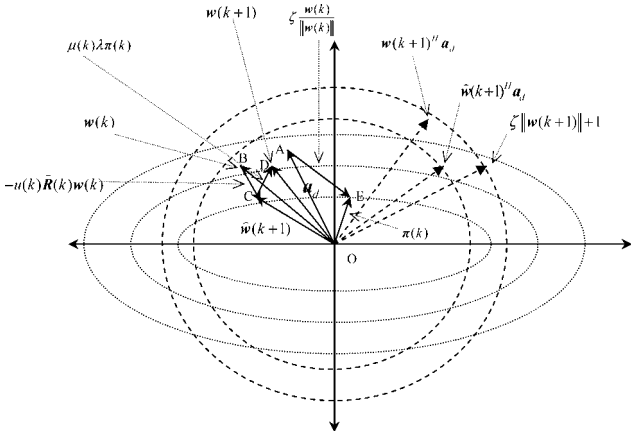


**Figure 1** *Geometric interpretation of the proposed ad hoc implementation*

## 5 Robust LCMV beamforming with MBWC constraints

The majority of the developed robust techniques in beamforming literature are based on single constraint in the desired look direction [3–10, 14–16]. Therefore if the desired source experiences multipath propagation and impinging on the antenna array from different angles associated with the dominant multipath rays, the robust technique with single constraint is not capable of gathering all multipath components, especially with large angular spread. Alternatively, the robust technique may concentrate only on the nominal AOI and neglect other components scattered in different multipaths which is not optimal in terms of optimising the output SINR. As a consequence, it is worthwhile to generalise the WC robust technique to include multiple constraints to form the robust LCMV beamformer with MBWC constraints analogous to the standard LCMV beamformer with MBC in (9). A generalisation for (18) with MBWC constraints can be expressed as

$$\begin{aligned} \min_{\breve{\boldsymbol{w}}} \quad & \breve{\boldsymbol{w}}^{\mathrm{H}}\widehat{\boldsymbol{R}}\breve{\boldsymbol{w}} \\ \text{subject to} \quad & \breve{\boldsymbol{w}}^{\mathrm{H}}\boldsymbol{\Lambda} \geq \boldsymbol{v}\left\|\breve{\boldsymbol{w}}\right\| + \boldsymbol{i} \end{aligned} \tag{37}$$

where $\Lambda$ is an $M \times N$ spatial matrix of the desired source, $\boldsymbol{v}$ a $1 \times N$ vector consisting of the WC constrained values and $\boldsymbol{i}$ a $1 \times N$ all-one vector where $N$ is the number of WC constraints (i.e. dominant multipath components, $N \leq L$). Then, a generalised cost function corresponding to (19) can be expressed as

$$\Theta(\boldsymbol{w}, \boldsymbol{\tau}) = \breve{\boldsymbol{w}}^{\mathrm{H}}\widehat{\boldsymbol{R}}\breve{\boldsymbol{w}} - \left(\breve{\boldsymbol{w}}^{\mathrm{H}}\boldsymbol{\Lambda} - \boldsymbol{v}\left\|\breve{\boldsymbol{w}}\right\| - \boldsymbol{i}\right)\boldsymbol{\tau} \tag{38}$$

where $\boldsymbol{\tau}$ is an $N \times 1$ vector of Lagrange multipliers. The step function is dropped due to *ad hoc* implementation. The following equations are corresponding to (26) and (28), respectively

$$\nabla = \frac{\partial\Theta(\breve{\boldsymbol{w}}, \boldsymbol{\tau})}{\partial\breve{\boldsymbol{w}}} = \widehat{\boldsymbol{R}}\breve{\boldsymbol{w}} - \left(\boldsymbol{\Lambda} - \boldsymbol{v}\left(\frac{\breve{\boldsymbol{w}}}{\|\breve{\boldsymbol{w}}\|}\right)\right)\boldsymbol{\tau} \tag{39}$$

$$\breve{\boldsymbol{w}}(k+1) = \tilde{\boldsymbol{w}}(k+1) + \mu(k)\bar{\boldsymbol{\Lambda}}\boldsymbol{\tau}(k) \tag{40}$$

where $\bar{\boldsymbol{\Lambda}} = \boldsymbol{\Lambda} - \boldsymbol{v}\left(\breve{\boldsymbol{w}}(k)/\left\|\breve{\boldsymbol{w}}(k)\right\|\right)$ is an $M \times N$ matrix and $\tilde{\boldsymbol{w}}(k+1) = \breve{\boldsymbol{w}}(k) - \mu(k)\widehat{\boldsymbol{R}}(k)\breve{\boldsymbol{w}}(k)$ is similar to $\widehat{\boldsymbol{w}}(k+1)$.

The vector of Lagrange multipliers is obtained by substituting (40) into the set of WC constraints in (37)

which engenders the following set of nonlinear equations

$$\left(\tilde{\boldsymbol{w}}(k+1)+\mu(k)\tilde{\boldsymbol{\Lambda}}\boldsymbol{\tau}(k)^{\mathrm{H}}\right)\boldsymbol{\Lambda} - \boldsymbol{v}\left\|\tilde{\boldsymbol{w}}(k+1)+\mu(k)\tilde{\boldsymbol{\Lambda}}\boldsymbol{\tau}(k)\right\| - \boldsymbol{i} = \boldsymbol{0} \tag{41}$$

where $\boldsymbol{0}$ is the all-zero vector. Unfortunately, a closed-form solution similar to (21) cannot be obtained because (41) is a system of nonlinear equations. In this case, a Newton-like method is obligatory to find the optimum vector of Lagrange multipliers $\boldsymbol{\tau}(k)$ that satisfies the set of WC constraints in (37). The trust region method [24, 25] is adopted to solve the system of nonlinear equations in (41). A minor drawback of this technique is that all WC constraints have to be solved via reducing them to equality if any of the WC constraints is not achieved.

The algorithm of the robust LCMV beamforming with MBWC consists of the following steps.

*Step 0.* Initialise $\widehat{\boldsymbol{R}}(0)=\boldsymbol{I}$, $\boldsymbol{w}(0)=\boldsymbol{a}_{\mathrm{d}}$, $\alpha=0.5$, $\eta=0.97$.

*Step 1.* Pick a new sample from array observations and compute the sample covariance matrix as $\widehat{\boldsymbol{R}}(k)=\eta\boldsymbol{R}(k-1)+\boldsymbol{x}(k)\boldsymbol{x}^{\mathrm{H}}(k)$; $M^2$.

*Step 2.* Compute the optimum step size using (36) where $\nabla \Leftarrow \boldsymbol{R}(k)\widetilde{\boldsymbol{w}}(k)$; $M^2+2M$.

*Step 3.* Update the unconstrained MV weight vector as $\tilde{\mathbf{w}}(k+1)=\widetilde{\boldsymbol{w}}(k)-\mu(k)\widehat{\boldsymbol{R}}(k)\widetilde{\boldsymbol{w}}(k)$; the matrix vector multiplication $\boldsymbol{R}(k)\boldsymbol{w}(k)$ is computed in step 2.

*Step 4.* If any $\left(\tilde{\boldsymbol{w}}(k+1)^{\mathrm{H}}\boldsymbol{\Lambda}\geq \boldsymbol{v}\|\tilde{\boldsymbol{w}}(k+1)\|+\boldsymbol{i}\right)$; $(MN+M)$ Compute $\boldsymbol{\tau}(k)$ by solving (41); $(2MN+M)(M+1)R$, where $R$ is the required number of iterations for the trust region method convergence.
Else $\boldsymbol{\tau}(k)=\boldsymbol{0}$ and $\widetilde{\boldsymbol{w}}(k+1)=\tilde{\boldsymbol{w}}(k+1)\rightarrow$ go to step 1.

*Step 5.* Update the weight vector of robust LCMV beamformer using (40) $\rightarrow$ Go to step 1.

As demonstrated in the above implementation, the robust LCMV beamformer with MBWC constraints requires $O\left(M^2(2NR+R+2)+M(2NR+N+R+3)\right)$ complexity. Indeed, it requires higher computational load; however, it cannot be compared with the single WC beamformers. Several simulation scenarios demonstrated that the trust region algorithm requires 4 to 12 iterations for convergence.

# 6 Numerical examples

A uniform linear array of $M=5$ omnidirectional sensors spaced half-wavelength apart is considered. All results are obtained by averaging 100 independent simulation runs. Through all examples, it is assumed that there is one desired source at 0° and two interfering sources at 45° and 60°. In the last two scenarios, a source with multipath propagation is considered. However, the main multipath component with dominant power is considered at 0°. The desired source is 5 dB power and each interference-to-noise ratio is equal to 10 dB. The noise power at each antenna element is equal to 0 dB to model a low SNR environment.

## 6.1 AOI mismatch scenario

In this scenario, the performance of the standard MVDR beamformer in (6) (referred to as standard MVDR), the robust MVDR beamformers with WC constraint which implemented using SOCP [5, 6] and eigendecomposition [4, 8] approaches (referred to, respectively, as robust MVDR-WC/SOCP and robust MVDR-WC/EigDec), and the proposed robust adaptive beamformer outlined in Section 4.2 (referred to as robust MVDR-WC/proposed) are compared. The aforementioned beamformers are simulated using a mismatched steering vector of the desired source where the presumed AOI equals 5°. The robust MVDR-WC/EigDec beamformer is computed using (22) and its norm is obtained using a Newton-like algorithm [4, 8]. In addition, the benchmark MVDR beamformer at (7) is simulated with the actual steering vector of the desired source. The benchmark MVDR beamformer is implemented using the well-known RLS algorithm. The update of the sample covariance matrix in (5) is used with all beamformers with $\eta=0.97$. The WC constrained parameter $\zeta=1.8$ is chosen for both robust MVDR-WC/EigDec and robust MVDR-WC/proposed beamformers, whereas $\zeta=3$ is chosen for robust MVDR-WC/SOCP beamformer. This is because the SOCP method is initialised with normalised weight vector [5, 6]. The WC constrained parameter is selected based on the best performance achieved from several simulation runs. In practical, it is selected based on some preliminary (coarse) knowledge about wireless channels or using Mont Carlo simulation. Fig. 2 shows the output SINR of the

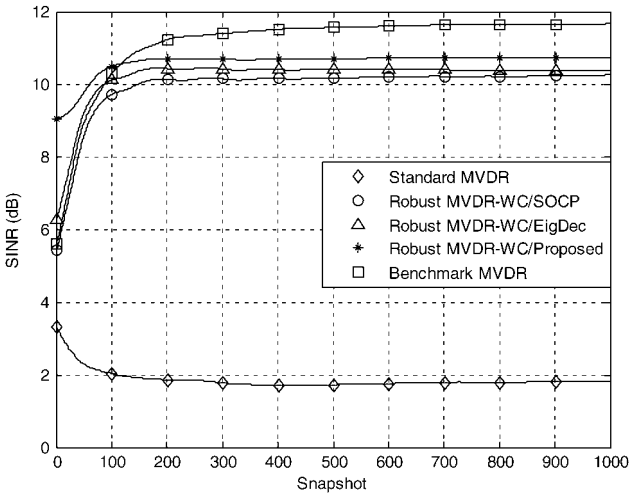


**Figure 2** *Output SINR against snapshot index for the first scenario*




doi: 10.1049/iet-spr:20070162

abovementioned beamformers against snapshot and beam patterns against AOI is illustrated in Fig. 3. The proposed algorithm offers the best SINR compared with other robust approaches and even faster convergence speed over the benchmark MVDR beamforming with the RLS algorithm. The eigendecomposition and SOCP methods are considered as batch algorithms where the weight vector of the robust MVDR-WC/EigDec beamformer is computed using the closed-form in (22) and the weight vector of the robust MVDR-WC/SOCP beamformer is recomputed completely with each snapshot [5]. Finally, the proposed algorithm is the best at eliminating sidlobes and interference compared with other robust approaches as evident from Fig. 3 where it is ranked after the Benchmark MVDR beamformer.

Fig. 4 shows the output SINR against noise power using 50 fixed training sample size (i.e. low sample support). The figure conspicuously demonstrates the superiority of the proposed beamformer especially at low noise power (i.e. high SNR) thanks to its optimality at low snapshot index as observed from Fig. 2.

In order to analyse the Lagrange multiplier in (34), the parameters of (33) which are given in (35) are investigated. These parameters and the Lagrange multiplier $\lambda$ (referred to as WC parameters) are plotted against snapshot index in Fig. 5 at $\zeta = 1.8$. The figure illustrates that $A > 0$, $B > 0$ and $C < 0$. Therefore (33) has one real positive root as explained in Section 4.1. It has to be noted that the algorithm commenced into the WC optimisation from the first snapshoot as shown in Fig. 5.

It is worthwhile to investigate the sensitivity of the proposed algorithm against the WC constrained value (i.e. $\zeta$). Fig. 6 demonstrates the performance of the proposed algorithm at several $\zeta$ values. It reveals that the

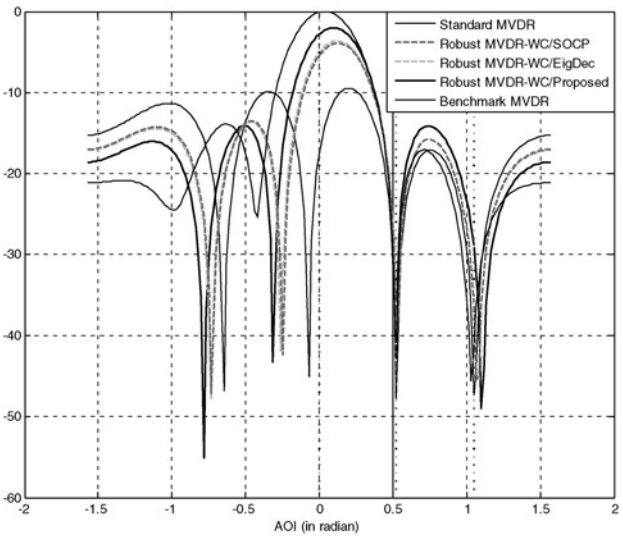


**Figure 3** *Steady-state array beam patterns against AOI (in radian) for the first scenario*

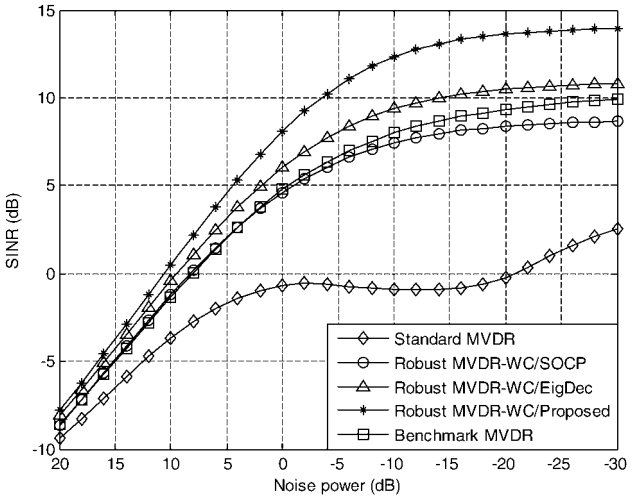


**Figure 4** *Output SINR against noise power for the first scenario with training data size $N = 50$*

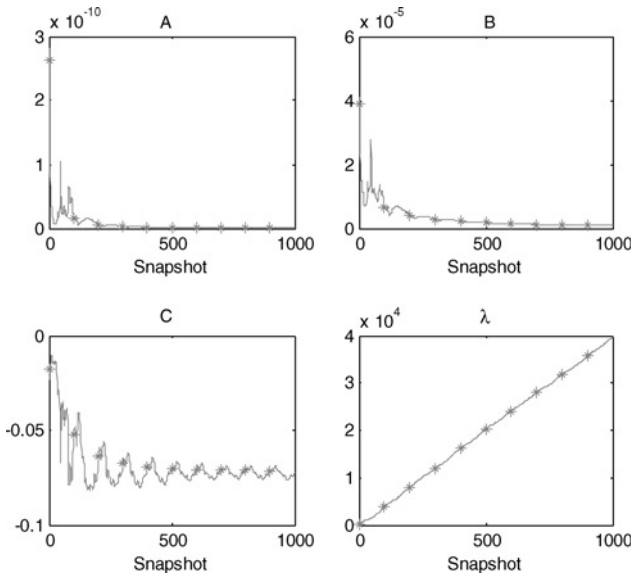


**Figure 5** *WC parameters of the robust MVDR-WC/proposed beamformer at $\zeta = 1.8$*

algorithm performs well at a reasonable window of $\zeta = [1.4{:}2.2]$ with optimality at $\zeta = 1.8$ in terms of start-up performance. Indeed, $\zeta$ is a crucial factor for any WC performance optimisation algorithm and it should be properly selected. As shown in Fig. 6, the algorithm starts to degrade when $\zeta$ is decreased because the algorithm is no longer capable of handling the mismatch degree. For clarity, the WC parameters at $\zeta = 1.2$ are illustrated in Fig. 7, which are almost analogous to Fig. 5 where $A > 0$, $B > 0$ and $C < 0$. However, the algorithm delays executing the WC optimisation because $\zeta$ is very low and subsequently the algorithm performance is degraded. More preciously, the algorithm executes the unconstrained MV minimisation without WC optimisation more than

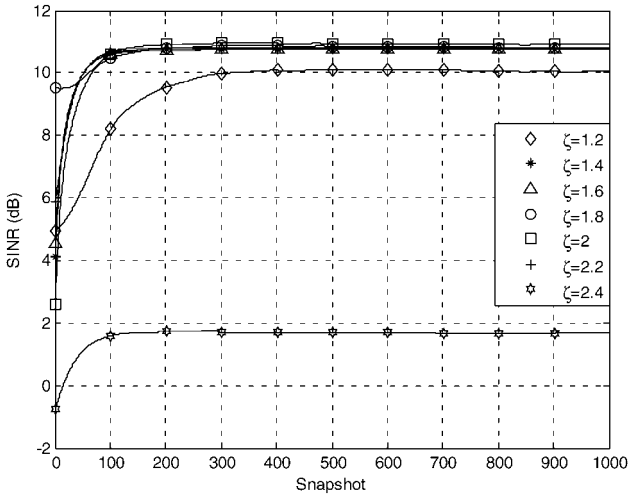


**Figure 6** *Effect of WC parameter ζ on the output SINR of the first scenario*

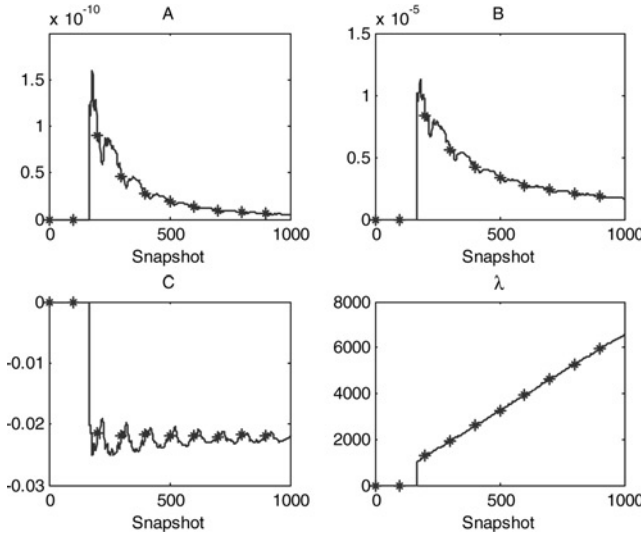


**Figure 7** *WC parameters of the robust MVDR-WC/ proposed beamformer at $\zeta = 1.2$*

necessary and hence a part of the interested signal is suppressed and it could not be recovered again with adaptive implementation.

Finally, the algorithm performance is seriously degraded when $\zeta$ is increased to 2.4 as shown in Fig. 8. The WC parameters at $\zeta = 2.4$ are shown in Fig. 8 which demonstrate that $A < 0, B > 0, C < 0$ and, in turn, (33) has one real positive root if $B^2 > AC$. Regrettably, the preceding condition could not be achieved where $|C| \gg 0$ and hence the solution of (33) has two complex roots and therefore the algorithm performance is seriously degraded. The plot of parameter $\lambda$ in Fig. 8 is only for real part. In order to avoid complex solution to (33), the WC constrained value $\zeta$ can be adjusted during adaptive

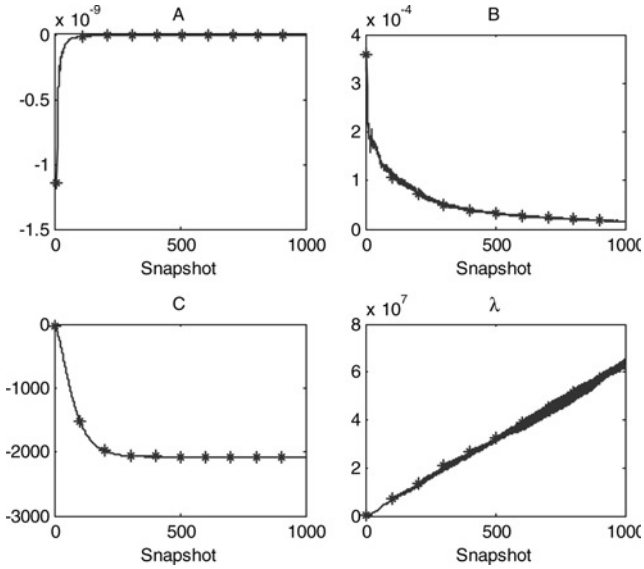


**Figure 8** *WC parameters of the robust MVDR-WC/ proposed beamformer at $\zeta = 2.4$*

implementation to guarantee that $A > 0$ and therefore the complex solution of (33) could be prevented. However, during initial iterations of some runs, one may have $A < 0$ while $B^2 > AC$ and therefore the algorithm can continue without adjusting $\zeta$. Consequently, the best practice is to verify if $A < 0$ and $B^2 < AC$ are met, and if so, $\zeta$ is decreased. The WC algorithm in Section 4.2 is revised by amending step 4 as follows.

*Step 4* If $\chi < \zeta\left|\widehat{\boldsymbol{w}}(k+1)\right|$, compute $\lambda$ using (34); $5M$.

If $\left(A < 0\left(B^2 < AC\right)\right)$, $\zeta = \zeta - 0.1$, end Else $\lambda = 0$ and $\boldsymbol{w}(k+1) = \widehat{\boldsymbol{w}}(k+1) \leftarrow$ go to step 1.

Another simulation is conducted to evaluate the performance of the above modified robust MVDR-WC/ proposed beamformer. The modified algorithm is initialised with the same parameters of the first scenario except that $\zeta = 3$. The WC parameters and the output SINR for the modified robust MVDR-WC/proposed beamformer are demonstrated in Figs. 9 and 10 respectively. Fig. 9 indicates that the algorithm starts with $A < 0, B > 0, C < 0$ and $B^2 < AC$ and then $\zeta$ starts to decrease until an acceptable value which prevent complex solution of (33).

## 6.2 Small angular spread scenario

In this scenario, a desired source with small angular spread emerging from multipath propagation as in rural cells is simulated. The same parameters of first scenario are used except that the SOI is impinging on the array from three directions associated with three multipath rays. There is a 5° mismatch with the dominant multipath ray. The other two rays amplitudes are 40% of the main component and they are impinging on the array from the directions 4° and −3°. The



doi: 10.1049/iet-spr:20070162

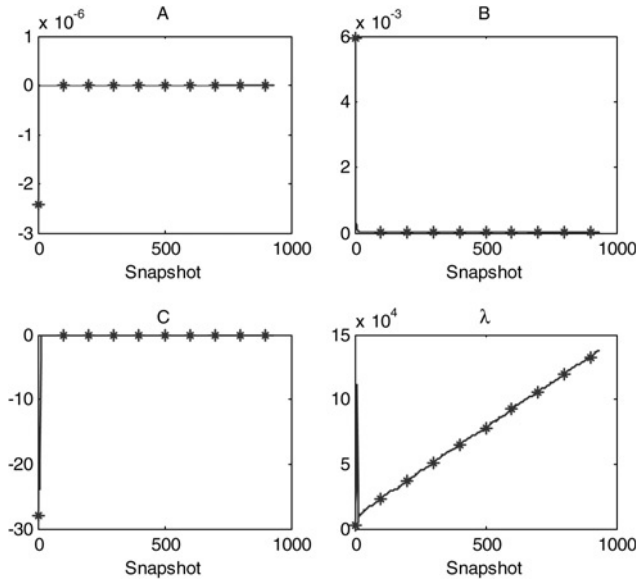


**Figure 9** *WC parameters of the modified robust MVDR-WC/proposed beamformer at $\zeta = 3$*

maximum angular spread (i.e. 4°) associated with the multipath components in this scenario is less than the AOI mismatch of the dominant multipath ray (i.e. 5°). In addition to the five beamformers simulated in the first scenario, the benchmark LCMV beamformer in (9) with MBC is simulated, which is imposed towards the three actual AOIs (i.e. 0°, 4°, −3°) of the multipath rays (referred to as benchmark LCMV). The multipath components in the benchmark LCMV beamformer are combined using MRC. The benchmark MVDR beamformer in (7) is simulated using only the actual steering vector of the dominant multipath ray. The WC parameter $\zeta$ of the robust beamformers is selected as in the first scenario. The performance of the aforesaid beamformers in terms of SINR is illustrated in Fig. 11. The proposed algorithm offers about 2 dB improvement over other robust approaches as evident from Fig. 11. The performance of the benchmark MVDR beamformer is degraded below the robust approaches, whereas the WC constraint bears the robust

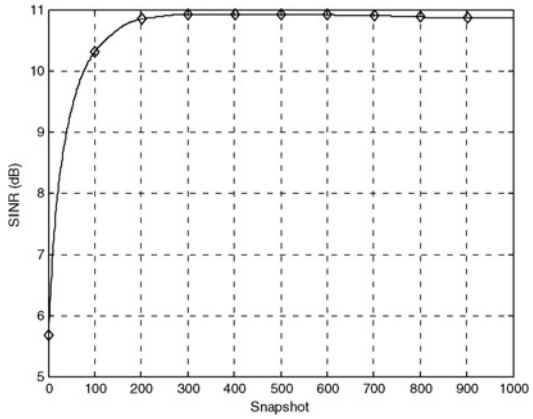


**Figure 10** *Output SINR against snapshot index for the modified robust MVDR-WC/proposed beamformer with the parameters of the first scenario*

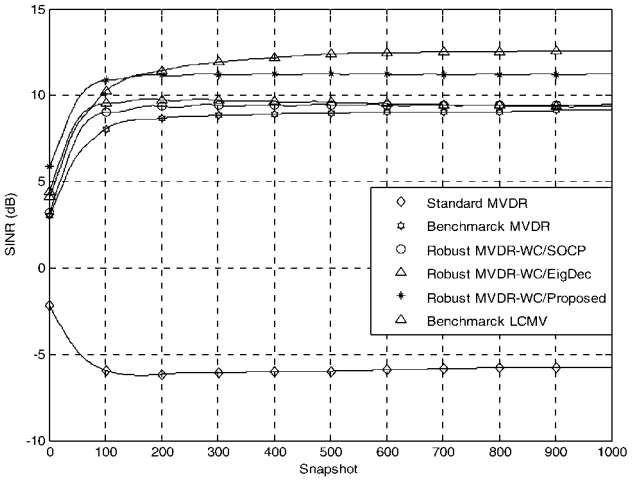


**Figure 11** *Output SINR against snapshot index for the second scenario*

beamformers by picking up some signal components from the multipath signals scattered inside the mismatch region bounded by $\zeta$.

## 6.3 Large angular spread scenario

In this scenario, a large angular spread as in the cellular indoor environment is simulated. The simulation system is similar to the previous scenario except that the three multipath components are impinging on the array from directions 0°, −30° and −80°. The dominant ray impinges on the array from 0° direction and there is a 5° look direction mismatch. It is assumed that the phases of the multipath rays are independently and uniformly drawn from the interval $[-\pi, \pi]$ in each run. The phases associated with multipaths vary from run to run and stay constant during adaptive implementation of each run. In this scenario, the beamformers in the previous experiments are simulated in addition to the proposed robust LCMV beamformer with MBWC constraints (referred to as robust LCMV-MBWC).

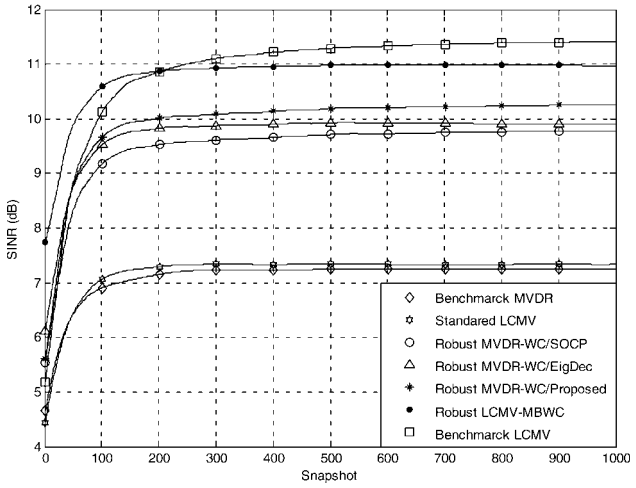


**Figure 12** *Output SINR against snapshot index for the third scenario*

Moreover, the standard LCMV beamformer with multiple constraints in (9) (referred to as standard LCMV) is simulated using a mismatched steering vector of the dominant multipath ray while there are no mismatches with the other two rays (i.e. $5^\circ$, $-30^\circ$, $-80^\circ$). The multipath rays of the benchmark LCMV and the standard LCMV beamformers are combined using MRC. The phases of multipath rays are unknown to all beamformers except the benchmark beamformers. The beamformers of the first scenario are simulated using the same parameters, whereas the robust LCMV-MBWC beamformer is simulated using $\boldsymbol{\upsilon} = [1.6 \quad 0.2 \quad 0.2]$. The selection of $\boldsymbol{\upsilon}$ is obtained practically using several simulation runs. It is somehow embodying the amplitude distribution of multipath rays. However, in-depth analysis for tuning this vector and even optimal estimation is a good candidate for future research. The SINR performance of the seven beamformers is demonstrated in Fig. 12. First of all, the benchmark LCMV is considerably degraded, despite tracing the dominant multipath ray. This is because the large angular spread deforms the effective steering vector of the SOI. The performances of the robust beamformers with the single WC constraint resemble their performances in the first scenario. The robust LCMV-MBWC beamformer offers about 1 dB improvement over the single WC constraint beamformers due to efficient multipath handling using multiple WC constraints.

## 7 Conclusions

In this paper, the robust adaptive beamforming using WC performance optimisation is implemented using novel *ad hoc* approaches. Two efficient implementations are developed using single and multiple WC constraints. The proposed implementations are based on iterative gradient minimisation. In contrast to the existing single WC robust approaches, the proposed single WC implementation requires very low computational load and it engenders the best performance, especially at low sample support. In addition, the proposed algorithm eliminates the covariance matrix inversion estimation. The WC performance optimisation is generalised to include multiple WC constraints which produce a robust LCMV beamformer with MBWC constraints. An efficient solution for the LCMV-MBWC beamformer is introduced by solving a system of nonlinear equations. Simulation results demonstrated the superiority of the proposed beamformers over the existing robust approaches. Future research may include fine-tuning of the constrained vector of the LCMV-MBWC beamformer and developing low complexity adaptive implementations.

## 8 References


[1] FELDMAN D.D., GRIFFITHS L.J.: 'A projection approach for robust adaptive beamforming', *IEEE Trans. Signal Process.*, 1994, **42**, (4), pp. 867–876

[2] GERSHMAN A.B.: 'Robust adaptive beamforming in sensor arrays', *AEU, Int. J. Electron. Commun.*, 1999, **53**, (6), pp. 305–314

[3] LI J., STOICA P.: 'Robust adaptive beamforming' (John Wiley & Sons, Inc, Hoboken, NJ, 2006)

[4] GERSHMAN A.B., LUO Z.-Q., SHAHBAZPANAHI S.: 'Robust adaptive beamforming based on worst-case performance optimization', in LI J., STOICA P. (EDS): 'Robust adaptive beamforming' (John Wiley & Sons, Inc, Hoboken, NJ, 2006), pp. 49–89

[5] VOROBYOV S.A., GERSHMAN A.B., LUO Z.-Q.: 'Robust adaptive beamforming using worst-case performance optimization: a solution to the signal mismatch problem', *IEEE Trans. Signal Process.*, 2003, **51**, (2), pp. 313–324

[6] CUI S., KISIALIOU M., LUO Z.-Q., DING Z.: 'Robust blind multiuser detection against signature waveform mismatch based on second order cone programming', *IEEE Trans. Wirel. Commun.*, 2005, **4**, (4), pp. 1285–1291

[7] SHAHBAZPANAHI S., GERSHMAN A.B.: 'Robust blind multiuser detection for synchronous CDMA system using worst-case performance', *IEEE Trans. Wirel. Commun*, 2004, **3**, (6), pp. 2232–2245

[8] ZARIFI K., SHAHBAZPANAHI S., GERSHMAN A.B., LUO Z.-Q.: 'Robust blind multiuser detection based on the worst-case performance optimization of the MMSE receiver', *IEEE Trans. Signal Process.*, 2005, **53**, (1), pp. 295–205

[9] ELNASHAR A.: 'Robust adaptive beamforming'. ACE2 Network of Excellence Workshop on Smart Antennas, MIMO Systems and Related Technologies, Mykonos, Greece, 8 June 2006

[10] LORENZ R.G., BOYD S.P.: 'Robust minimum variance beamforming', *IEEE Trans. Signal Process.*, 2005, **53**, (5), pp. 1684–1696

[11] BESSON O., VINCENT F.: 'Performance analysis of beamformers using generalized loading of the covariance matrix in the presence of random steering vector errors', *IEEE Trans. Signal Process.*, 2005, **53**, (2), pp. 452–459

[12] VINCENT F., BESSON O.: 'Steering vector errors and diagonal loading', *IEE Proc., Radar Sonar Navig.*, 2004, **151**, (6), pp. 337–343

[13] STURM J.F.: 'Using SeDuMi 1.02, a MATLAB toolbox for optimization over symmetric cones', *Optim. Methods Softw.*, 1999, **11–12**, pp. 625–653

[14] SHAHBAZPANAHI S., GERSHMAN A.B., LUO Z.Q., WONG K.M.: 'Robust adaptive beamforming for general-rank signal model', *IEEE Trans. Signal Process.*, 2003, **51**, (9), pp. 2257–2269




doi: 10.1049/iet-spr:20070162

[15] ELNASHAR A., ELNOUBI S., ELMIKATI H.: 'Further study on robust adaptive beamforming with optimum diagonal loading', *IEEE Trans. Antennas Propag.*, 2006, **54**, (12), pp. 3647–3658

[16] LI J., STOICA P., WANG Z.: 'On robust Capon beamforming and diagonal loading', *IEEE Trans. Signal Proces.*, 2003, **51**, (7), pp. 1702–1715

[17] ELNASHAR A., ELNOUBI S., ELMIKATI H.: 'Robust adaptive beamforming with variable diagonal loading'. Proc. 6th IEE Int. Conf. 3G & Beyond (3G 2005), London, UK, November 2005, pp. 489–493

[18] ERTEL R.B., CARDIERI P., SOWERBY K.W., RAPPAPORT T.S., REED J.H.: 'Overview of spatial channel models for antenna communication systems', *IEEE Pers. Commun.*, 1998, **5**, (1), pp. 10–22

[19] VAN DER VEEN A.-J.: 'Algebraic methods for deterministic blind beamforming', *Proc. IEEE*, 1998, **86**, (10), pp. 1987–2008

[20] TIAN Z., BELL K.L., VAN TREES H.L.A.: 'Recursive least squares implementation for LCMP beamforming under quadratic constraint', *IEEE Trans. Signal Process.*, 2001, **49**, (6), pp. 1138–1145

[21] ATTALLAH S., ABED-MERAIM K.: 'Fast algorithms for subspace tracking', *IEEE Trans. Signal Process. Lett.*, 2001, **8**, (7), pp. 203–206

[22] ELNASHAR A., ELNOUBI S., EL-MAKATI H.: 'Performance analysis of blind adaptive MOE multiuser receivers using inverse QRD-RLS algorithm', *IEEE Trans. Circuits Syst. I*, 2008, **55**, (1), pp. 398–411

[23] CHOI S., SHIM D.: 'A novel adaptive beamforming algorithm for smart antenna system in a CDMA mobile communication environment', *IEEE Trans. Veh. Technol.*, 2000, **49**, (5), pp. 1793–1806

[24] POWELL M.J.D.: 'A Fortran subroutine for solving systems of nonlinear algebraic equations', in RABINOWITZ P. (ED.): 'Numerical methods for nonlinear algebraic equations' (Gordon and Breach Science Publishers, New York, 1988)

[25] CONN N.R., GOULD N.I.M., TOINT PH.L.: 'Trust-region methods' MPS/SIAM series on optimization' (SIAM and MPS, 2000)